

# Synthetic Molecular Motors: Thermal N Inversion and Directional Photoinduced C=N Bond Rotation of Camphorquinone Imines

Lutz Greb, Andreas Eichhöfer, and Jean-Marie Lehn\*

**Abstract:** The thermal and photochemical *E/Z* isomerization of camphorquinone-derived imines was studied by a combination of kinetic, structural, and computational methods. The thermal isomerization proceeds by linear *N* inversion, whereas the photoinduced process occurs through C=N bond rotation with preferred directionality as a result of diastereoisomerism. Thereby, these imines are arguably the simplest example of synthetic molecular motors. The generality of the orthogonal trajectories of the thermal and photochemical pathways allows for the postulation that every suitable chiral imine qualifies, in principle, as a molecular motor driven by light or heat.

Non-equilibrium processes and their coupling to directed nanoscopic, microscopic, and, ultimately, macroscopic displacements are intrinsic to life. Such tasks are usually performed by biological macromolecules and have been perfected over millions of years.<sup>[1]</sup> To unravel the basic molecular mechanisms of directional displacement, it is constructive to start with the simplest/smallest possible molecular devices. Small-molecule systems acting as artificial molecular machines and motors, with a 1000 times smaller molecular weight than biological motor proteins, can be classified by their mode of action (for example rotation, walking, contraction).<sup>[2–4]</sup> Among the most intensively studied synthetic molecular motors are the light-driven unidirectional rotating overcrowded olefins.<sup>[3]</sup> By fine adjustment of their steric or electronic parameters, it has been shown in a striking number of derivatives that the factors influencing the rotational frequency of such motors are well understood and can be tuned.<sup>[4]</sup> Such devices have been shown to indeed effect macroscopic changes by their coupling to surfaces or to hydrogels.<sup>[5]</sup> Nevertheless, the field of light-driven rotating molecular motors with functionalities other than olefins remains little explored.

We demonstrated recently that a four-step mode of displacement of the rotor part around the stator could be accomplished by using the special features of chiral imines, easily synthesized in a one-step procedure starting from

commercial compounds.<sup>[6]</sup> The directionality was verified by following the fate and interconversion of the diastereomeric states A/A'/B/B' (Figure 1a). More importantly, pursuing a conjecture based on the orthogonality of the thermal and photochemical configurational switching of imines, those motors were tuned to have a two-step mode of action, depending on the nature of the stator part and the N sub-

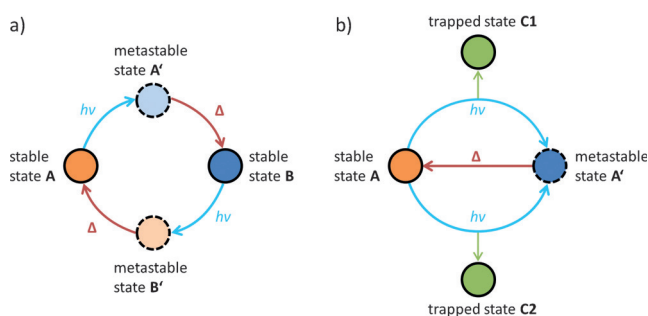


**Figure 1.** Schematic comparison of a) a four-step and b) a two-step motor.

stituent (Figure 1b; A/A').<sup>[7]</sup> This mode of action is intrinsically accessible only by imines and consists of a photochemical out-of-plane C=N bond rotation and a thermal in-plane *N* inversion. The thermal process has experimentally<sup>[8]</sup> and theoretically<sup>[9]</sup> been proven to be a linear *N* inversion, whereas the photochemical C=N bond isomerization has been only theoretically confirmed to be a rotational process, both in the  $S_2$  ( $\pi \rightarrow \pi^*$ ) and in the  $S_1$  ( $n \rightarrow \pi^*$ ) state.<sup>[10]</sup> The directionality is based on the assumption that the photochemical C=N bond rotation should exhibit preferred directionality due to displacement through diastereotopic subspaces spanned by chirality in the molecule, and thus ensuing unsymmetrical excited-state surfaces. Thus, the two-step mode-of-action should impart a motor-like motion, based on analogy with the behavior of olefinic double bonds and on theoretical considerations and plausibility. If imines with chirality at a suitable distance indeed undergo a photochemical C=N bond rotation with preferred directionality, consequently every suitable chiral imine would qualify as a molecular motor. This essential question remains to be unambiguously answered.

Direct experimental proof of the photoinduced trajectory is precluded by the fast dynamics in the excited state. It is thus necessary to gain insight into the photochemical C=N bond rotation by indirect methods. Trapping of a photochemically generated species on its rotational pathway in the two different diastereoisomers would indicate a preferred direc-

[\*] Dr. L. Greb, Prof. Dr. J.-M. Lehn  
Institut de Science et d'Ingénierie Supramoléculaires (ISIS)  
Université de Strasbourg, 8 allée Gaspard Monge  
Strasbourg 67000 (France)  
E-mail: lehn@unistra.fr

Dr. L. Greb, Dr. A. Eichhöfer  
Institut für Nanotechnologie (INT)  
Karlsruhe Institut für Technologie, Hermann-von-Helmholtz-Platz 1  
76344 Eggenstein-Leopoldshafen (Germany)

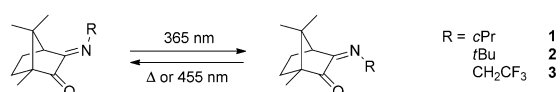
Supporting information for this article is available on the WWW under <http://dx.doi.org/10.1002/ange.201506691>.

tionality of rotation (Figure 1 b; trapped states). Indeed, the observation of diastereoselectivity in the *N*-cyclopropylimin-1-pyrroline photo-rearrangement of chiral *N*-cyclopropylbenzylidene imines was originally used to elucidate the underlying mechanism and it was concluded by comparison of experimental and theoretical results that a biased rotation around the C=N bond plays the decisive role.<sup>[11]</sup>

Herein, we present a new class of synthetic imine molecular motors, incorporating the natural product camphor and its corresponding chirality, as essentially the simplest example of a synthetic molecular motor. Identification of the thermal *N* inversion pathway is supported by kinetic analysis of the thermal isomerization in comparison with X-ray molecular structures and computed transition-state energies. The directionality in the photochemical C=N bond isomerization is investigated by trapping of biradical intermediates in a *N*-cyclopropylimin-1-pyrroline photo-rearrangement. The orthogonality of the thermal and photochemical pathways thus highlights chiral imines as a unique class of molecular motors.

The camphorquinone-derived imines (**1–3**) were synthesized by TiCl<sub>4</sub>-mediated condensation of commercially available (*R*)-(-)-camphorquinone with suitable amines (specifically *tert*-butyl-, cyclopropyl-, or 2,2,2-trifluoroethylamines) to obtain the desired products in good yields (Scheme 1).<sup>[12,13]</sup> <sup>1</sup>H-NOESY NMR and X-ray crystallographic structure analysis confirmed the *E* configuration of the imines as the thermodynamically favored compounds (Figure 2).

Irradiation of solutions of imines with UV light at  $\lambda = 365$  nm in CD<sub>3</sub>CN resulted in the formation of photostationary states (PSSs) containing imines in the *Z* configuration in 64–79% yield (Table 1). The yellow-colored *Z* isomers were entirely converted back into the *E* isomers upon irradiation with blue light ( $\lambda = 455$  nm). The switching could be cycled up to ten times without significant side reactions, thus characterizing these imines as new two-way photo-switches. The thermal *Z*-to-*E* back-isomerization was investigated by time- and temperature-dependent <sup>1</sup>H NMR spectroscopy, yielding free energies of activation ( $\Delta G^\ddagger$ ) ranging from circa 21–25 kcal mol<sup>-1</sup>. The relative thermal stability of the *Z* isomers of **1** and **2** was markedly different (at 293 K,



**Scheme 1.** Photochemical and thermal isomerization of camphorquinone imines. cPr = cyclopropyl.

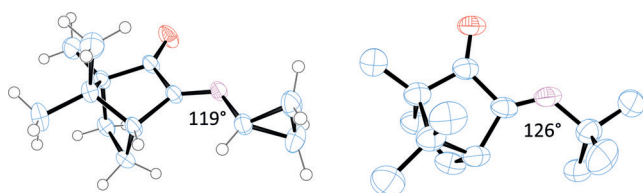


**Figure 2.** Molecular structures of imines **1** (left) and **2** (right). Values given are the C=N–C bond angles. Atom colors: C = blue; H = white; O = red; N = pink.

**Table 1:** Thermodynamic, kinetic, photochemical, and calculated transition-state energies of **1–3**.

| Imine  | <b>1</b><br>(R = cyclopropyl) | <b>2</b><br>(R = <i>t</i> Bu) | <b>3</b><br>(R = CH <sub>2</sub> CF <sub>3</sub> ) |
|--|-------------------------------|-------------------------------|--|
| <i>E/Z</i> (thermal)   | 92:8                          | 99:1                          | 82:18  |
| <i>E/Z</i> (PSS at 365 nm) <sup>[a]</sup>                          | 36:64                         | 21:79                         | 29:71  |
| <i>E/Z</i> (PSS at 455 nm) <sup>[b]</sup>                          | 99:1                          | 99:1                          | 99:1   |
| $\Delta H^\ddagger$ [kcal mol <sup>-1</sup> ]                      | 24.7 ± 0.6                    | 22.8 ± 0.5                    | 19.0 ± 0.8   |
| $\Delta S^\ddagger$ [e.u.]   | –1.1 ± 0.05                   | 5.7 ± 0.2                     | –19.7 ± 1.9  |
| $\Delta G^\ddagger$ [293] [kcal mol <sup>-1</sup> ]                | 24.7                          | 21.2                          | 24.7   |
| calc. $\Delta E^\ddagger$ [kcal mol <sup>-1</sup> ] <sup>[c]</sup> | 24.2                          | 21.7                          | 25.6   |

[a] Measured using a UV handlamp (6 W,  $\lambda = 365$  nm) irradiating for 5 h.

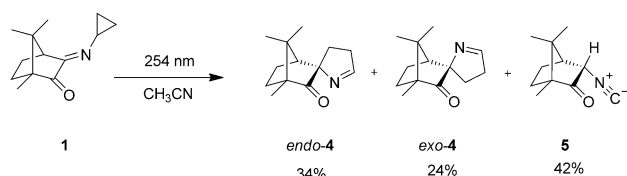
[b] Measured using a LED (5 W,  $\lambda = 455$  nm) irradiating for 1 h.

[c] Calculated electronic energies for linear transition states at the B2PLYP-D3/def2-TZVP level + COSMO solvent correction. For further details, see the Supporting Information.

half-life  $\tau_{1/2} = 10$  min for **2**, 7.5 h for **1**). This difference would not be expected if solely electronic factors were considered, and instead indicates a steric ground-state destabilization for **2**. Accordingly, the molecular structure of **2** shows a noticeable enlargement of the C=N–C bond angle (126°) compared to the less bulky and thermally more stable **1** (119°; Figure 2).

Interestingly, no significant torsion (pre-twist) around the C=N bond was detected in either case, in agreement with a linear *N* inversion pathway on the ground-state surface. The activation entropies for **1** and **2** were small and concentration independent, indicative of unimolecular processes. The lower activation enthalpy and notably negative activation entropy of **3** may be rationalized in terms of *n*-to- $\sigma^*$  hyperconjugation of the nitrogen lone pair to the  $\sigma^*$  (C–CF<sub>3</sub>) orbital.<sup>[14]</sup> This hyperconjugation would lead to stabilization of the transition state but only in one over three possible conformations, thus reducing the rotational degrees of freedom. Structures and energies of both configurational isomers and transition states were calculated by means of DFT (B2PLYP-D3/def2-TZVP/COSMO).<sup>[15]</sup> The calculated bond angles and bond lengths are in good agreement with the available X-ray solid-state molecular structures and the relative energies of the isomers reflect the preference for the *E* isomers. The transition-state structures along the ground-state surface correspond in all cases to a linear C=N–C geometry. The calculated energies fit with the experimentally determined energies for the thermal *Z*-to-*E* back-isomerization of compounds **1–3** (Table 1), thus confirming the *N* inversion pathway in the ground state.

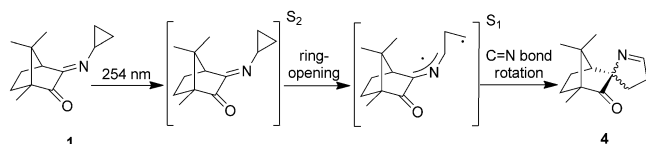
Irradiation of a solution of the *N*-cyclopropylimine **1** in CH<sub>3</sub>CN or D<sub>2</sub>O with light of shorter wavelength ( $\lambda = 254$  nm) than necessary for *E/Z* isomerization ( $\lambda = 365$  nm) effected the photochemical *N*-cyclopropylimin-1-pyrroline rearrangement (Scheme 2). The product distribution of the crude mixture was determined by integration of the signals in the <sup>1</sup>H NMR spectrum for the imines and more accurately by gas chromatography. The rearrangement reaction was performed on a preparative scale (200 mg). The products were isolated and their structures were confirmed by two-dimensional <sup>1</sup>H-COSY, <sup>1</sup>H-NOESY, HSQC, and HMBC NMR spectra. In addition to the expected pyrroline products **4**, ethylene gas (<sup>1</sup>H NMR signal at  $\delta = 5.41$  ppm) was formed as well as isonitrile **5** (42%; confirmed by X-ray crystallographic



**Scheme 2.** Photochemical *N*-cyclopropylimin-1-pyrroline rearrangement of **1**.

structure determination), most likely by a photoinduced [2+2] cycloreversion reaction.<sup>[16,17]</sup> Most importantly, the two diastereomeric spirocyclic pyrroline products *endo*-**4**/*exo*-**4** were obtained with an unbalanced d.r. value of 58:42, also indicating a preferred directionality in the C=N bond rotation (see below).

Our assignment of the singlet nature of the excited states for *E/Z* isomerization ( $\lambda = 365$  nm) and photo-rearrangement ( $\lambda = 254$  nm) was supported by the photoreaction of **1** in the presence of a 10-fold excess of piperylene, without a significant loss in efficiency.<sup>[18]</sup> In analogy to the literature,<sup>[11]</sup> we consider that upon irradiation with light at  $\lambda = 254$  nm, the  $S_2$  state leads to the opening of the cyclopropyl ring to give a biradical before reaching the  $S_1/S_2$  conical intersection ( $CI_{S_2/S_1}$ ; Scheme 3). Thereafter, the pathway chosen on the



**Scheme 3.** Proposed ring opening and diastereoselective ring closure after biased C=N bond rotation.

$S_1$  surface, causing the C=N bond rotation, is guided by the relative energies along the rotation vectors through the diastereomeric spaces, reflected in the ratio obtained in the final diastereospecific ring closing of the biradical. Importantly, besides the photo-rearrangement to the pyrroline, *E/Z* isomerization took place at  $\lambda = 254$  nm with much higher efficiency. The photostationary state at  $\lambda = 254$  nm (*E/Z* ratio = 48:53) was reached within 30 minutes of irradiation whereas the complete conversion to **4/5** for the same sample took 3 hours. The Frank–Condon regions and corresponding relaxation pathways in the excited state should be different in shape, depending on whether they are reached from the *E* or the *Z* ground-state isomer. It can be assumed that the preferred direction of rotation is different from both sides, and that the observed d.r. value (58:42) is a lower-limit level reflecting the PSS (48:53), hence concealing a higher inherent selectivity. In other words, it is likely that if every excitation event commenced solely from the *E* isomer, a higher selectivity might be expected. Indeed, when the reaction was performed with a medium-pressure mercury lamp in  $D_2O$  (irradiating with light of wavelengths over the complete UV/Vis spectrum), the observed diastereomeric ratio for *endo*-**4**/*exo*-**4** increased to 68:32. Irradiation with

light from the visible part of the electromagnetic spectrum led to formation of a PSS with an *E/Z* ratio of 78:22. Consequently, the probability that a molecule now starting from the *E* isomer reaches the  $S_2$  state, with subsequent reaction to form *endo*-**4**, might be increased, as reflected in a higher diastereomeric ratio.

Applied in the context of molecular motors, the *N*-cyclopropyl imine rearrangement serves as a tool to investigate directionality in the photoinduced C=N bond rotation and should generally allow quantification of the efficiency of imine molecular motors (and more precisely of the stator parts). Of course, it must be noted that the rotational pathway of the intermediate open-shell biradical species (from the  $S_2$  state) may have a different selectivity than that of the pure C=N bond rotation (from the  $S_1$  state), but it should nevertheless serve as a guiding value.

The present work gives insight into the unique orthogonal trajectories of thermal and photochemical isomerization of chiral imines, finally providing experimental support for the original conjecture.<sup>[7]</sup> The camphorquinone-derived imines (or other small-molecule chiral imines)<sup>[19]</sup> are arguably the simplest prototypical example of synthetic molecular motors. The thermal *N* inversion is confirmed by kinetic analysis in combination with molecular structures and calculated energies of the transition states. The diastereospecific trapping of biradical intermediates provides support for the directional photochemical C=N bond rotation. Consequently, every chiral imine could serve potentially as a molecular motor in response to light and heat, driven by light as the cleanest fuel and relaxing towards thermal equilibrium.

## Acknowledgements

L.G. thanks the Alexander von Humboldt foundation for a postdoctoral fellowship. We also thank the ERC (Advanced Research Grant SUPRADAPT 290585) for financial support. Exploratory experiments have been performed by Dr. Nema Hafezi on another type of system. We thank Prof. Stefan Bräse for sharing the Rayonet Photoreactor.

**Keywords:** density functional calculations · imines · isomerization · molecular motors · photochemistry

**How to cite:** *Angew. Chem. Int. Ed.* **2015**, *54*, 14345–14348  
*Angew. Chem.* **2015**, *127*, 14553–14556

- [1] a) M. Schliwa, *Molecular motors*, Wiley-VCH, Weinheim, **2003**; b) M. Schliwa, G. Woehlke, *Nature* **2003**, *422*, 759–765.
- [2] a) J.-P. Sauvage, V. Amendola, *Molecular machines and motors*, Springer, Berlin, **2001**; b) T. R. B. V. Kelly, *Molecular machines*, Springer, Berlin, **2005**; c) E. R. Kay, D. A. Leigh, F. Zerbetto, *Angew. Chem. Int. Ed.* **2007**, *46*, 72–191; *Angew. Chem.* **2007**, *119*, 72–196; d) A. Credi, S. Silvi, M. Venturi, W. R. Browne, *Molecular machines and motors: recent advances and perspectives*, Springer, Berlin, **2014**; e) D.-H. Qu, Q.-C. Wang, Q.-W. Zhang, X. Ma, H. Tian, *Chem. Rev.* **2015**, *115*, 7543–7588.
- [3] N. Koumura, R. W. J. Zijlstra, R. A. van Delden, N. Harada, B. L. Feringa, *Nature* **1999**, *401*, 152–155.
- [4] a) M. M. Pollard, M. Klok, D. Pijper, B. L. Feringa, *Adv. Funct. Mater.* **2007**, *17*, 718–729; b) M. Klok, N. Boyle, M. T. Pryce, A.

- Meetsma, W. R. Browne, B. L. Feringa, *J. Am. Chem. Soc.* **2008**, *130*, 10484–10485; c) M. M. Pollard, A. Meetsma, B. L. Feringa, *Org. Biomol. Chem.* **2008**, *6*, 507–512; d) A. S. Lubbe, N. Ruangsupapichat, G. Caroli, B. L. Feringa, *J. Org. Chem.* **2011**, *76*, 8599–8610; e) J. Bauer, L. Hou, J. C. M. Kistemaker, B. L. Feringa, *J. Org. Chem.* **2014**, *79*, 4446–4456.
- [5] a) T. Kudernac, N. Ruangsupapichat, M. Parschau, B. Macia, N. Katsonis, S. R. Harutyunyan, K.-H. Ernst, B. L. Feringa, *Nature* **2011**, *479*, 208–211; b) Q. Li, G. Fuks, E. Moulin, M. Maaloum, M. Rawiso, I. Kulic, J. T. Foy, N. Giuseppone, *Nat. Nanotechnol.* **2015**, *10*, 161–165.
- [6] L. Greb, J.-M. Lehn, *J. Am. Chem. Soc.* **2014**, *136*, 13114–13117.
- [7] J.-M. Lehn, *Chem. Eur. J.* **2006**, *12*, 5910–5915.
- [8] a) H. Kessler, D. Leibfritz, *Tetrahedron* **1970**, *26*, 1805–1820; b) H. Kessler, D. Leibfritz, *Tetrahedron Lett.* **1970**, *11*, 1423–1426; c) H. Kessler, *Tetrahedron* **1974**, *30*, 1861–1870; d) R. Knorr, J. Ruhdorfer, J. Mehlstäubl, P. Böhler, D. S. Stephenson, *Chem. Ber.* **1993**, *126*, 747–754.
- [9] a) J. M. Lehn, B. Munsch, *Theor. Chim. Acta* **1968**, *12*, 91–94; b) R. Macaulay, L. A. Burnelle, C. Sandorfy, *Theor. Chim. Acta* **1973**, *29*, 1–7; c) H. Yamataka, S. C. Ammal, T. Asano, Y. Ohga, *Bull. Chem. Soc. Jpn.* **2005**, *78*, 1851–1855; d) A. Gaenko, A. Devarajan, L. Gagliardi, R. Lindh, G. Orlandi, *Theor. Chem. Acc.* **2007**, *118*, 271–279; e) J. Gálvez, A. Guirado, *J. Comput. Chem.* **2010**, *31*, 520–531; f) S. He, Y. Tan, X. Xiao, L. Zhu, Y. Guo, M. Li, A. Tian, X. Pu, N.-B. Wong, *J. Mol. Struct. Theochem.* **2010**, *951*, 7–13.
- [10] a) P. Russegger, *Chem. Phys.* **1978**, *34*, 329–339; b) Y. Osamura, S. Yamabe, K. Nishimoto, *Int. J. Quantum Chem.* **1980**, *18*, 457–462; c) P. Russegger, *Chem. Phys. Lett.* **1980**, *69*, 362–366; d) V. Bonacic-Koutecky, M. Persico, *J. Am. Chem. Soc.* **1983**, *105*, 3388–3395; e) V. Bonačić-Koutecký, J. Michl, *Theor. Chim. Acta* **1985**, *68*, 45–55; f) I. Tavernelli, U. F. Röhrig, U. Rothlisberger, *Mol. Phys.* **2005**, *103*, 963–981.
- [11] a) P. J. Campos, A. Soldevilla, D. Sampedro, M. A. Rodríguez, *Org. Lett.* **2001**, *3*, 4087–4089; b) A. Soldevilla, D. Sampedro, P. J. Campos, M. A. Rodríguez, *J. Org. Chem.* **2005**, *70*, 6976–6979; c) D. Sampedro, A. Soldevilla, M. A. Rodríguez, P. J. Campos, M. Olivucci, *J. Am. Chem. Soc.* **2005**, *127*, 441–448.
- [12] For experimental details, see the Supporting Information.
- [13] S. E. Denmark, I. Rivera, *J. Org. Chem.* **1994**, *59*, 6887–6889.
- [14] T. Asano, H. Furuta, H. J. Hofmann, R. Cimiraglia, Y. Tsuno, M. Fujio, *J. Org. Chem.* **1993**, *58*, 4418–4423.
- [15] For computational details, see the Supporting Information.
- [16] a) H. Quast, G. Meichsner, *Chem. Ber.* **1987**, *120*, 1049–1058; b) H. Quast, A. Fuß, A. Heublein, H. Jakobi, B. Seiferling, *Chem. Ber.* **1991**, *124*, 2545–2554.
- [17] For X-ray solid-state molecular structure and a proposed mechanism, see the Supporting Information. CCDC 1411350 (**1**), 1411351 (**2**), and 1411352 (**5**) contain the supplementary crystallographic data for this paper. These data are provided free of charge by The Cambridge Crystallographic Data Centre.
- [18] As a result of the concurrent thermal *E/Z* isomerisation and experimental requirements, the exact determination of quantum yields was not pursued.
- [19] The imines reported in Ref. [11 c] are not molecular motors since the stereoinformation in those derivatives is lost by very fast racemization of the chiral cyclopropyl rings.

Received: July 20, 2015

Published online: October 9, 2015